British Journal of Pharmacology (2001) 134, 1787–1795

www.nature.com/bjp

Evidence for two endothelin Et_A receptor subtypes in rabbit arteriolar smooth muscle

[1]Tim M. Curtis & *,[1]C. Norman Scholfield

[1]Smooth Muscle Group, Department of Physiology, Queens University, 97 Lisburn Road, Belfast, BT9 7BL

1 Effects of endothelin-1 (Et-1) were studied on membrane currents in choroidal arteriolar smooth muscle by using perforated patch-clamp recordings.

2 Et-1 (10 nM) activated oscillatory Ca^{2+}-activated Cl^--currents ($I_{Cl(Ca)}$) which could not be reversed by washing out.

3 Currents through L-type Ca^{2+} channels were resolved in a divalent free medium ($I_{Ca(L)Na}$). Et-1 reduced $I_{Ca(L)Na}$ by $75\pm7\%$ within 30 s and this effect faded over 5 min, when the depression remained constant. On washing out Et-1, $I_{Ca(L)Na}$ almost completely recovered within 10 s.

4 BQ123 (1 μM), a peptide Et_A receptor blocker, prevented the activation of $I_{Cl(Ca)}$, but failed to inhibit $I_{Cl(Ca)}$ transients once they had been initiated. In contrast, BQ123 not only prevented but also reversed the inhibition of $I_{Ca(L)Na}$ by Et-1. BQ788 (1 μM), an Et_B receptor antagonist, did not prevent the activation of $I_{Cl(Ca)}$ or the inhibition of $I_{Ca(L)Na}$ by Et-1.

5 ABT-627 (10 nM), a non-peptide Et_A receptor antagonist also blocked the activation of $I_{Cl(Ca)}$. However, on $I_{Ca(L)Na}$, ABT-627 (10 nM) mimicked the action of Et-1 an effect blocked by BQ123 suggesting that ABT-627 acted as an agonist.

6 The data are consistent with choroidal arteriolar smooth muscle cells having two types of Et_A receptor, one where BQ123 is an antagonist and ABT-627 an agonist, where ligands dissociate freely and this receptor is coupled to inhibition of L-type Ca^{2+} channels. In the other, BQ123 and ABT-627 are both antagonists and with Et-1 the receptor converts to a high affinity state producing the classical irreversible activation $I_{Cl(Ca)}$.

British Journal of Pharmacology (2001) **134,** 1787–1795

Keywords: Endothelin-1; Et_A receptors; Calcium-activated chloride channels; L-type calcium channels; arteriolar smooth muscle; ABT-627

Abbreviations: $[Ca^{2+}]_i$, intracellular calcium concentration; Et-1, endothelin-1; $I_{Ca(L)Na}$, sodium current carried through L-type calcium channels; $I_{Cl(Ca)}$, Calcium-activated chloride current

Introduction

Endothelin-1 (Et-1) is a potent vasoconstrictor peptide that is produced by the vascular endothelium (Yanagisawa *et al*., 1988). In the ocular circulation, Et-1 has attracted some attention because of its possible role in microvascular disease including diabetic retinopathy (de la Rubia *et al*., 1992; Chakravarthy *et al*., 1994; Bursell *et al*., 1995; McGinty *et al*., 1999). It may also mediate in other vascular diseases including stroke (Pluta *et al*., 1997; Lampl *et al*., 1997), chronic heart failure and renal vascular disease (Webb *et al*., 1998).

So far, two types of endothelin-receptors have been characterized in mammalian tissues, namely Et_A and Et_B receptors (Arai *et al*., 1990; Sakurai, *et al*., 1990). Both receptor types belong to the heptahelical receptor superfamily and couple *via* G-proteins to multiple intracellular effectors. Et_B receptors exist as subtypes, Et_{B1} and Et_{B2}. In the vascular bed, Et_A and Et_{B2} receptors co-exist on smooth muscle cells and mediate contraction, while endothelial cells possess Et_{B1} receptors which modulate the release of relaxing factors such as nitric oxide and prostacyclin.

*Author for correspondence at: Department of Ophthalmology, Institute of Clinical Science, Royal Victoria Hospital, Belfast, BT12 6BA; E-mail: N.SCHOLFIELD@QUB.AC.UK

The contractile action of Et-1 is peculiar compared to most vasoconstrictors. Contractions develop slowly, they are sustained and are virtually irreversible. This irreversibility has been attributed to an extremely slow rate of dissociation of Et-1/Et receptor complex. In rabbit choroidal arteriolar smooth muscle, Et-1 invariably produces a persistent elevation in cell Ca^{2+} resulting from increased Ca^{2+} influx. This may be partly attributed to the activation of a store-operated Ca^{2+} channel which is not voltage activated but is dihydropyridine-sensitive (Curtis & Scholfield, 2001). This increase in Ca^{2+} not only leads directly to contraction but also activates Cl^- channels which may affect Ca^{2+} entry (Curtis & Scholfield, 2000). This peptide can abolish L-type Ca^{2+} current in other microvascular smooth muscle (Guibert & Beech, 1999). Likewise, in a preliminary study we showed that Et-1 blocked L-type Ca^{2+} channels in choroidal arteriolar smooth muscle, although the time-course of the changes were dissimilar (Curtis & Scholfield, 1999). More interestingly, however, we discovered that the kinetics of Et-1 action on the Cl^- and L-type Ca^{2+} channels were radically different. In the present experiments we aim to show that this effect arises from the activation of two functionally distinct Et_A receptor subtypes.

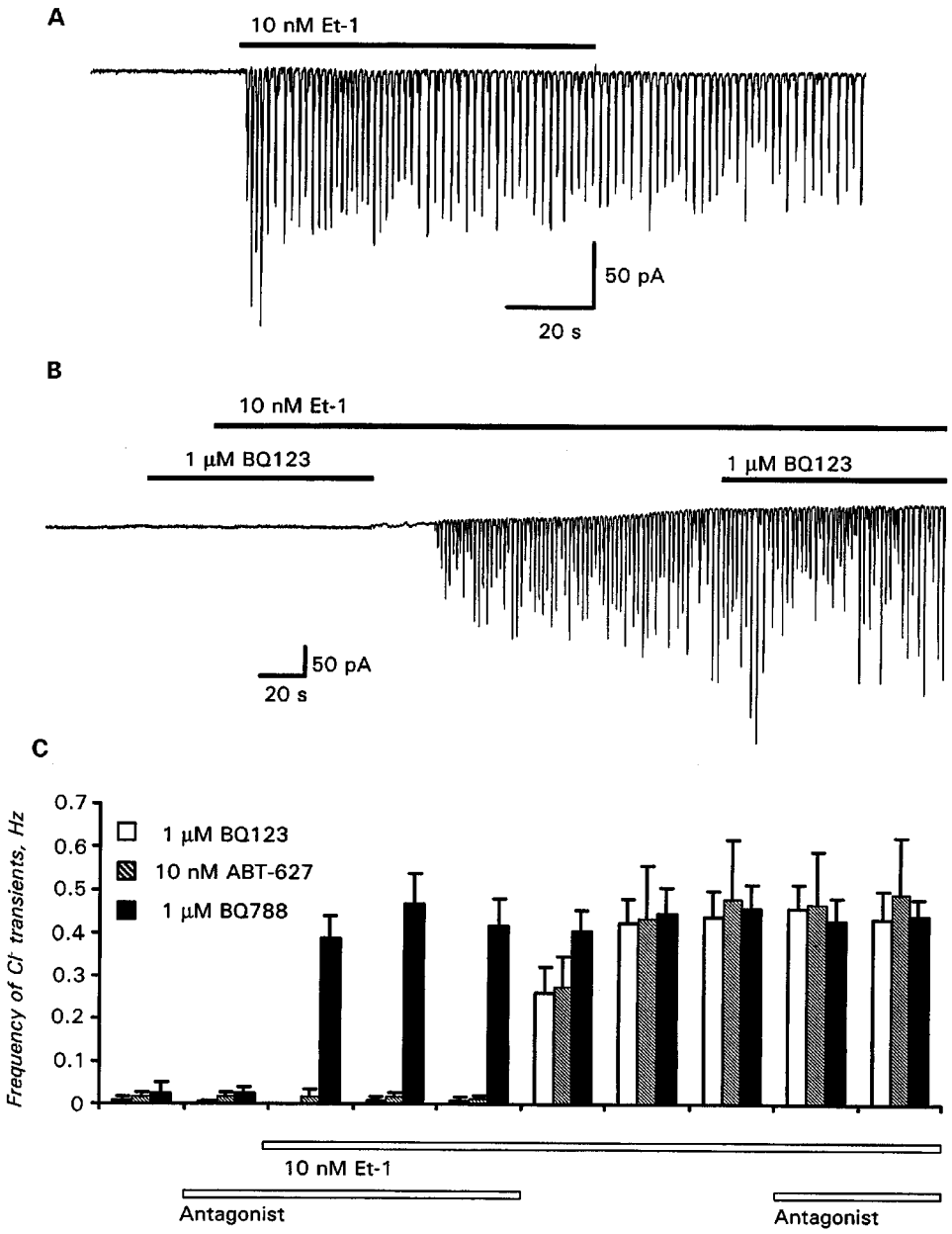

Figure 1 $I_{Cl(Ca)}$ transients with Et-1. (A) Current record showing the effect of Et-1 (10 nM) applied extracellularly to a choroidal arteriolar fragment held at −80 mV. This peptide activated oscillations of inward current, which we have previously characterized as being mediated by Ca^{2+}-activated Cl^- channels. Washing out the Et-1 from the bathing medium failed to reverse the rhythmical inward currents. (B) Voltage clamp record for a vessel fragment held at −80 mV showing the effect of the Et_A receptor antagonist BQ123 (1 μM). BQ123 prevents the Et-1 induction of $I_{Cl(Ca)}$, but fails to inhibit the current oscillations once they have been initiated. (C) Summary histograms (1 min periods) for the protocol adopted in B using the antagonists BQ123 ($n=6$), ABT-627 ($n=5$) or BQ788, ($n=5$).

Methods

Tissue dispersion

The eyes were removed from New Zealand white rabbits (2–4 kg) of either sex, freshly killed by sodium pentobarbitone overdose (80 mg kg^{-1}; injected into an ear vein). The eyeballs were bisected, the retinas removed and discarded, and the choroids peeled away and sliced into pieces (1–4 mm^2) in Ca^{2+}-free solution. After 30 min in Ca^{2+}-free solution at 15°C, the tissue was incubated for 10 min at 34°C in solution containing 20 μM Ca^{2+} and 0.05 mg ml^{-1} trypsin (Sigma, Poole, U.K.). It was then re-suspended in 20 μM Ca^{2+} solution with 0.2 mg ml^{-1} collagenase type 1A (Sigma, Poole, U.K.) and incubated at 34°C for 20 min. During the enzyme incubations a magnetic stirring bar continuously agitated the tissue and dispersion of vessel segments achieved by trituration of the suspension with a fire-polished Pasteur pipette. The homogenate was centrifuged at 1000 r.p.m. for 1 min and the supernatant was discarded. The fragments were re-suspended in 50 μM Ca^{2+} solution and stored for 30 min at 4°C. Finally, the isolated vessels were centrifuged

again and maintained in 100 μM Ca^{2+} solution at 4°C. They remained viable for >6 h. Recordings were made from single cells still embedded within microvessel fragments. These fragments were 25–60 μm in length, 40–50 μm in width and contained up to 15 smooth muscle cells. In some experiments, single smooth muscle cells were isolated by longer collagenase digestion at 37°C.

Electrophysiology

Dispersed fragments were allowed to settle on the bottom of a 2 ml recording bath on the stage of an inverted microscope (Eclipse TE200, Nikon) for 10 min. Normal solution was then allowed to flow into one end of the bath and withdrawn from the other at 2 ml min^{-1}. The solution passed through a heat exchanger such that cells in the recording bath were at 36°C. Drug solutions were delivered through a separate tube (350 μm in diameter by 6 mm in length) long enough to allow temperature equilibration with the bath solution. The delivery tube was positioned approximately 200 μm away from the vessel under study, and was fed by a seven-way manifold leading from seven separate reservoirs each controlled by valve. The delay time for new solution to reach a cell was 1 s as measured by switching to dye solution.

Membrane currents were recorded using the perforated patch configuration of the whole cell patch-clamp technique (Horn & Marty, 1988; Hamill *et al*., 1981). Electrodes (1–2 MΩ) were pulled from filamented borosilicate glass capillaries (1.5 mm o.d. × 1.17 mm i.d., Clark Electromedical Instruments, U.K.) with a Flaming-Brown micropipette puller (Model P-87, Sutter Instruments, U.S.A.). Recordings were made using an Axopatch-1D patch-clamp amplifier (Axon Instruments, U.S.A.). Internal pipette solutions were K^+ based with amphotericin B as the perforating agent. Experimentation was delayed until full perforation of the membrane patch had been accomplished which usually took 3–5 min. Liquid junction potentials (<2 mV) were compensated electronically, but series resistance (10–15 MΩ) and cell capacitance (25–70 pF) were usually uncompensated. For experiments using square step protocols, leakage currents were subtracted on-line. From a holding potential of −80 mV, the correction signal was obtained by averaging three hyperpolarizing steps (−30, −20 and −10 mV from the holding voltage), a procedure that did not activate ion channels, but allowed measurement of passive membrane properties and leak. Data were low pass filtered at 0.5 kHz and sampled digitally at 2 kHz by an National Instruments PC1200 interface and stored on disk for off-line analysis using software provided by Dempster, J., University of Strathclyde, U.K. (Version 2.1). Choroidal arteriole segments of up to 100 μm in length can be homogeneously space-clamped (Curtis & Scholfield, 2001). Hence, the segments used in the current experiments (up to 60 μm in length) were uniformly voltage-clamped. Some single cells were recorded in whole cell patch mode using a solution without amphotericin.

Solutions

The bathing solution contained (in mM): NaCl 120, KCl 5, D-glucose 5, $CaCl_2$ 2, $MgCl_2$ 1.3, HEPES 10, pH 7.3 with NaOH. For Ca^{2+}-free solution, the $CaCl_2$ was omitted and adding the appropriate amount of $CaCl_2$ made low Ca^{2+} solutions. Both Ca^{2+} and Mg^{2+} were omitted for the divalent-free solution and 5 mM EGTA was added. For Na^+-free divalent free medium NaCl was replaced by equimolar N-Methyl-D-glucamine (NMDG) and pH was adjusted with HCl. Recording electrodes contained (in mM): KCl 52, Kgluconate 80, $MgCl_2$ 1, EGTA 0.5, HEPES 10, pH 7.2 to which 200 μg ml^{-1} amphotericin B was added. For conventional whole-cell recordings the pipette solution contained (in mM): Kgluconate 140, HEPES 10, $MgCl_2$ 1, EGTA 0.5, ATP (2 Na) 2, Phosphocreatine (2 Na) 2, GTP (2 Na) 0.1, $CaCl_2$ 1.3, pH 7.2 with KOH. All voltage-clamp experiments were done in the presence of 20 mM tetraethylammonium (TEA) in order to block outward K^+ currents.

Amphotericin B, TEA, nifedipine, (±) Bay K8644, BQ788 and tetrodotoxin were purchased from Sigma (Poole, U.K.). Endothelin-1 (human, porcine) came from Tocris (Bristol, U.K.) and BQ123 was obtained from American Peptide Co (California, U.S.A.). ABT-627 was provided by Dr Jerry Wassale of Abbot Laboratories, Michigan, U.S.A.

Accumulated data are expressed as means ± s.e.mean, and unless otherwise stated statistical differences were compared using the paired *t*-test (two-tailed), taking the $P<0.05$ level as significant.

Results

In the first series of experiments, vessel segments were voltage-clamped at −80 mV and 10 nM Et-1 was applied. In all six vessels examined regular transient inward currents were generated within 5–7 s of adding Et-1 (Figure 1A). Once activated by Et-1 the repetitive inward currents were continuously generated. Both the frequency and amplitudes of the currents were maintained for periods of up to 2 h (end of experiment) regardless of whether or not Et-1 was still present, i.e. the effect of Et-1 never washed out ($n=6$). Previously, we have characterized these Et-1 evoked currents as being mediated by Ca^{2+}-activated Cl^- channels because (i) their reversal potentials were influenced by changes in $[Cl^-]_i$; they were (ii) rapidly blocked by the Cl^- channel blockers niflumic acid and anthracene-9-carboxylic acid; (iii) lost in low Cl^- bathing medium; (iv) enhanced when I^- was substituted for Cl^-; and (v) abolished in Ca^{2+}-free medium (Curtis & Scholfield, 2000).

In the vasculature two Et receptor subtypes have been identified, Et_A and Et_B and in choroidal arteriolar smooth muscle Et_A receptors predominate (Stitt *et al*., 1996). In the presence of the selective Et_A receptor antagonist BQ123 (1 μM), Et-1 did not give rise to any transient Ca^{2+}-activated Cl^- currents (Figure 1B,C). However, when BQ123 was washed out with solution still containing Et-1, current pulses were generated following a delay of 27 ± 2 s. Once Et-1 had elicited these repetitive Ca^{2+}-activated Cl^- currents re-applying BQ123 (for up to 15 min) would not reverse them (Figure 1B,C). Similar results were attained using ABT-627 (10 nM), a non-peptide Et_A receptor blocker (Figure 1C). The selective Et_B receptor antagonist, BQ788 (1 μM) failed to prevent the activation of $I_{Cl(Ca)}$ by Et-1 (Figure 1C).

Ca^{2+} current through L-type channels was very small in choroidal arteriolar smooth muscle bathed in 2 mM Ca^{2+}

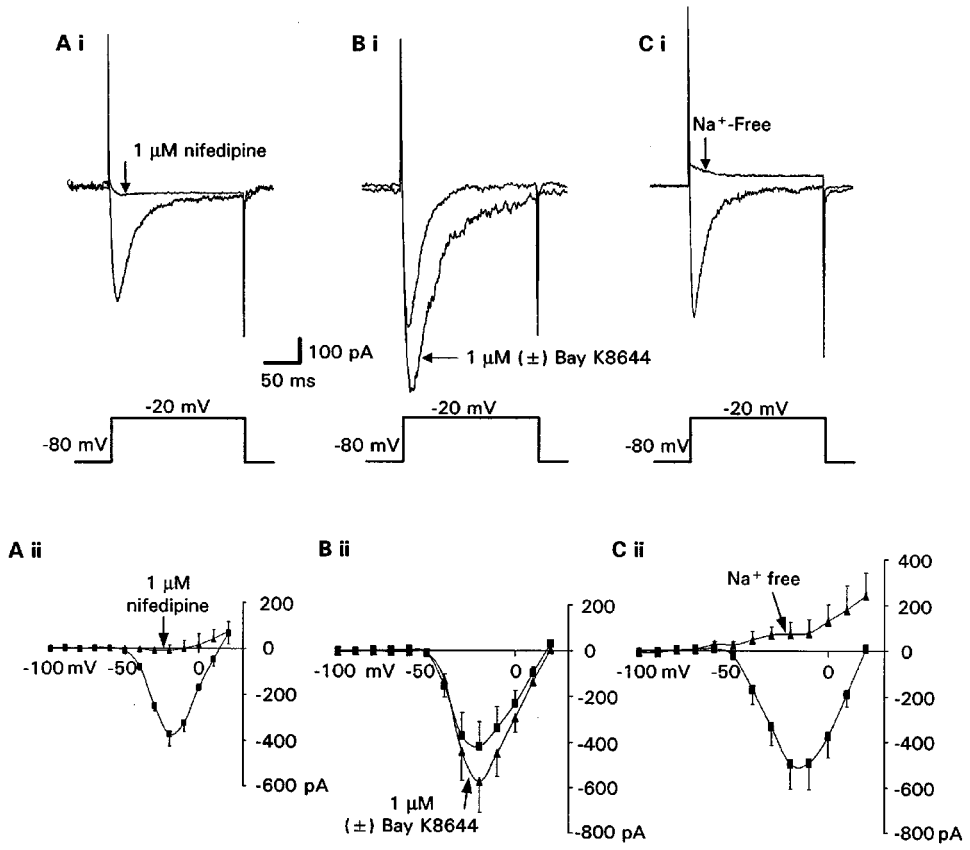

Figure 2 $I_{Ca(L)Na}$ in choroidal arteriolar smooth muscle. Current flowing through L-type Ca^{2+} channels was recorded in a divalent free medium. (Ai) Currents recorded in response to a voltage step from −80 to −20 mV before and after bath application of the L-type Ca^{2+} channel blocker nifedipine (1 μM). (Aii) The *I-V* relationships of the inward current first in normal bathing medium and then in 1 μM nifedipine ($n=6$). (Bi) Currents recorded using the same protocol as in Ai prior to and after Bay K8644 (1 μM), an L-type Ca^{2+} channel agonist. (Bii) Summary *I-V* plots showing the efficacy of Bay K8644 action across a range of voltages ($n=6$). (Ci & Cii) Na^+-free divalent free medium abolished the inward current. Results from five vessel fragments are pooled in Cii.

(~0.3 pA/pF) reflecting a low density of Ca^{2+} channels (Curtis & Scholfield, 2001). Therefore all of the following experiments were performed in a divalent-free medium to create a manageable current amplitude and to prevent interference by the Ca^{2+}-dependent Cl^- current (which is activated by Ca^{2+} influx through L-type Ca^{2+} channels in vascular smooth muscle) (McDonald *et al*., 1994; Large & Wang, 1996).

In divalent free solution vessel segments were held at −80 mV and subjected to 200 ms test pulses ranging between −100 mV and +20 mV. Steps to potentials more positive than −50 mV evoked a fast inward current, which peaked within 10 ms (Figure 2Ai,ii). The current grew to a maximal amplitude of −374±51 pA ($n=6$) at −20 mV, and became smaller with progressively stronger depolarizing pulses (Figure 2Aii). This inward current was characterized as being Na^+-influx through L-type Ca^{2+} channels ($I_{Ca(L)Na}$) since it was (i) abolished by 1 μM nifedipine (Figure 2Ai,ii); (ii) enhanced by 1 μM (±) Bay K8644 (Figure 2Bi,ii); (iii) absent in Na^+-free divalent free medium (Figure 2Ci,ii); and (iv) unaffected by 1 μM tetrodotoxin ($n=5$; data not shown). With test steps from −80 mV to −20 mV every 15 s, the amplitude of $I_{Ca(L)Na}$ remained constant for periods ⩾15 min ($n=6$).

In all but three out of 65 vessels tested, 10 nM Et-1 inhibited $I_{Ca(L)Na}$. In 39 of the vessels this was sustained, while in the remaining vessels the inhibition (⩾80%) lasted for <2 min and was not repeatable even after 10 min washout of Et-1. The particular response observed could not be ascribed to differences in vessel diameter (unpaired *t*-test). Only vessels showing a prolonged reduction of $I_{Ca(L)Na}$ were studied in further detail.

The time course for the sustained inhibition of $I_{Ca(L)Na}$ by Et-1 is illustrated in Figure 3Ai,ii. In 12 vessels, the depressant effect of Et-1 on $I_{Ca(L)Na}$ was maximal within 30 s of its addition to the bathing solution (peak current reduced by 75±7%). Over the next 5 min, the inhibition of $I_{Ca(L)Na}$ by Et-1 steadied out to 54±8%, where it then remained constant. Within 10 s of washing out Et-1, $I_{Ca(L)Na}$ recovered to 5% of its original value. After the spontaneous partial recovery of $I_{Ca(L)Na}$ and subsequent washout, Et-1 was re-applied. This time, the depression of $I_{Ca(L)Na}$ was smaller than a naïve addition and corresponded to the level of depression attained after 5 min application of Et-1. *I-V* curves show that Et-1 reduced the amplitude of $I_{Ca(L)Na}$ over most voltage ranges (Figure 3B), but this reduction was less pronounced for voltage steps more positive than −20 mV.

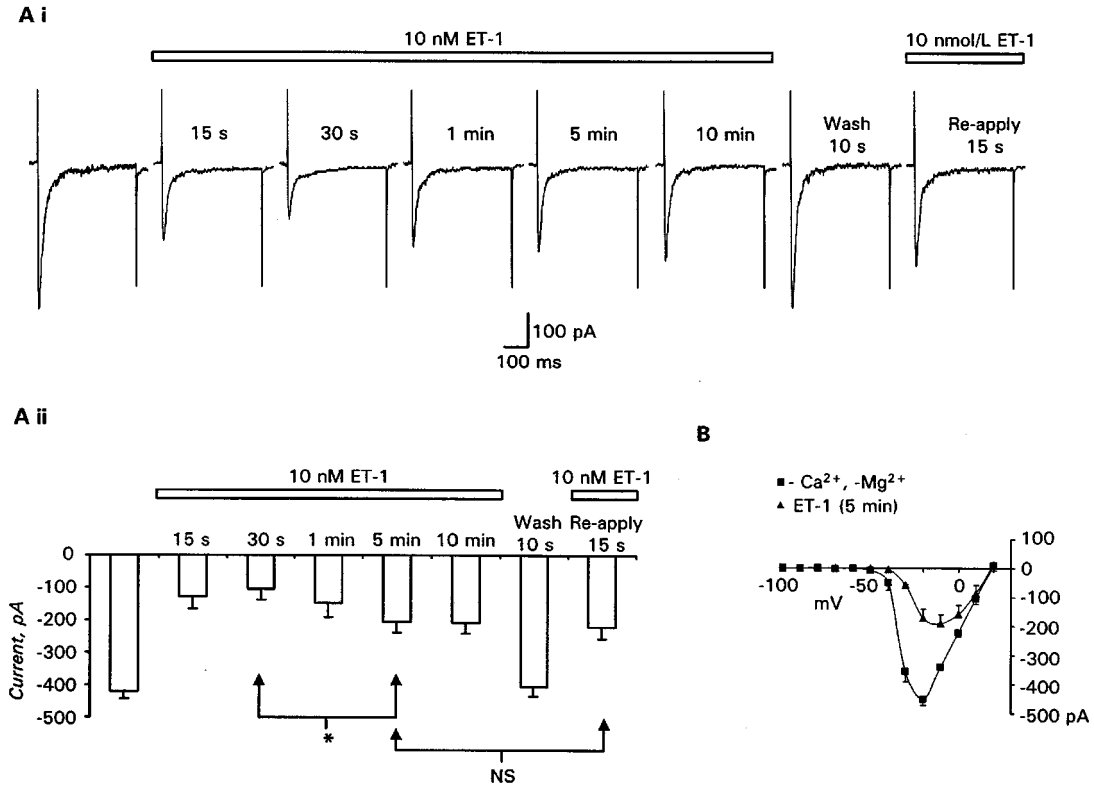

Figure 3 Time course and voltage dependence for the inhibition of $I_{Ca(L)Na}$ by Et-1 (Ai) Successive current traces recorded from a choroidal arteriolar fragment bathed in divalent free solution in response to voltage steps from −80 mV to −20 mV before, during, following washout and then re-application of 10 nM Et-1. (Aii) A histogram from 12 similar experiments showing peak $I_{Ca(L)Na}$ at −20 mV. *refers to a $P<0.05$ for 5 min Et-1 compared to 30 s Et-1 and NS signifies a $P>0.05$ for 15 s re-application of Et-1 versus 5 min Et-1. (B) *I-V* relationship showing the voltage dependence of the block of $I_{Ca(L)Na}$ during 5 min exposure to 10 nM Et-1 ($n=6$).

To eliminate the possibility that Et-1 was directly blocking L-type Ca^{2+} channels, experiments were performed on single isolated arteriolar smooth muscle cells using both perforated patch and conventional whole-cell recording methods. Experiments in the perforated patch configuration yielded results similar to those described for the vessel segments above, with a $59\pm7\%$ inhibition of $I_{Ca(L)Na}$ 5 min after adding 10 nM Et-1 ($n=5$). In contrast, no appreciable block of $I_{Ca(L)Na}$ was observed with Et-1 when conventional whole-cell recordings were made ($n=6$; $P>0.05$). Furthermore, Ca^{2+}-microfluorimetry experiments on single cells and vessel segments (Curtis & Scholfield, 2001) showed no persistent rise in $[Ca^{2+}]_i$ following application of Et-1 in divalent free solution ($n=6$ per group). The above results imply that the Et-1 induced inhibition of $I_{Ca(L)Na}$ in choroidal arteriolar smooth muscle is not due to direct channel blockade and is not *via* Ca^{2+}-mediated inactivation of the channels. Instead, the block appears to take place *via* a second messenger pathway which can be washed away when experiments are carried out using conventional whole-cell recording methods.

To characterize the Et receptor involved in the Ca^{2+} channel inhibition, the Et_A receptor antagonist BQ123 (1 μM) was tested on vessel segments. Initially we examined whether BQ123 was capable of preventing the sustained inhibition of $I_{Ca(L)Na}$ by Et-1. Because some vessels would not react to Et-1 in this manner (see above), it was necessary to firstly confirm a sustained block (for 5 min) of $I_{Ca(L)Na}$ with Et-1 prior to testing the effects of the antagonist. When Et-1 was washed out for 20 s the current recovered. BQ123 was then applied for 1 min and finally the solution was switched to one containing both Et-1 and the antagonist (Figure 4A,Bi). No changes in the amplitude of $I_{Ca(L)Na}$ were observed in the presence of BQ123 alone or with BQ123 and Et-1. In contrast, the Et_B receptor antagonist, BQ788 (1 μM) failed to prevent the sustained inhibition of $I_{Ca(L)Na}$ by Et-1 (Figure 4Bii). The next series of experiments tested whether or not BQ123 could reverse the blockade of Ca^{2+} channels by Et-1. After 5 min sustained inhibition of $I_{Ca(L)Na}$ by Et-1, BQ123 was applied to the bathing medium with Et-1 still present (Figure 4C). The inhibition of $I_{Ca(L)Na}$ was briskly reversed with the peak current returning to an amplitude similar to that observed prior to the conditioning dose of Et-1 after 60 s.

To further characterize the Et receptor involved in the Ca^{2+} channel inhibition, the non-peptide Et_A receptor blocker ABT-627 was tested. However, we found that ABT-627 (10 nM) by itself inhibited $I_{Ca(L)Na}$ in a manner similar to that observed with Et-1. The time course for the inhibition of $I_{Ca(L)Na}$ by ABT-627 is shown in Figure 5A. As with Et-1, the maximal inhibition of $I_{Ca(L)Na}$ occurred within 30 s of its application to the bathing solution and this effect then diminished over the next 10 min and was fully reversed on

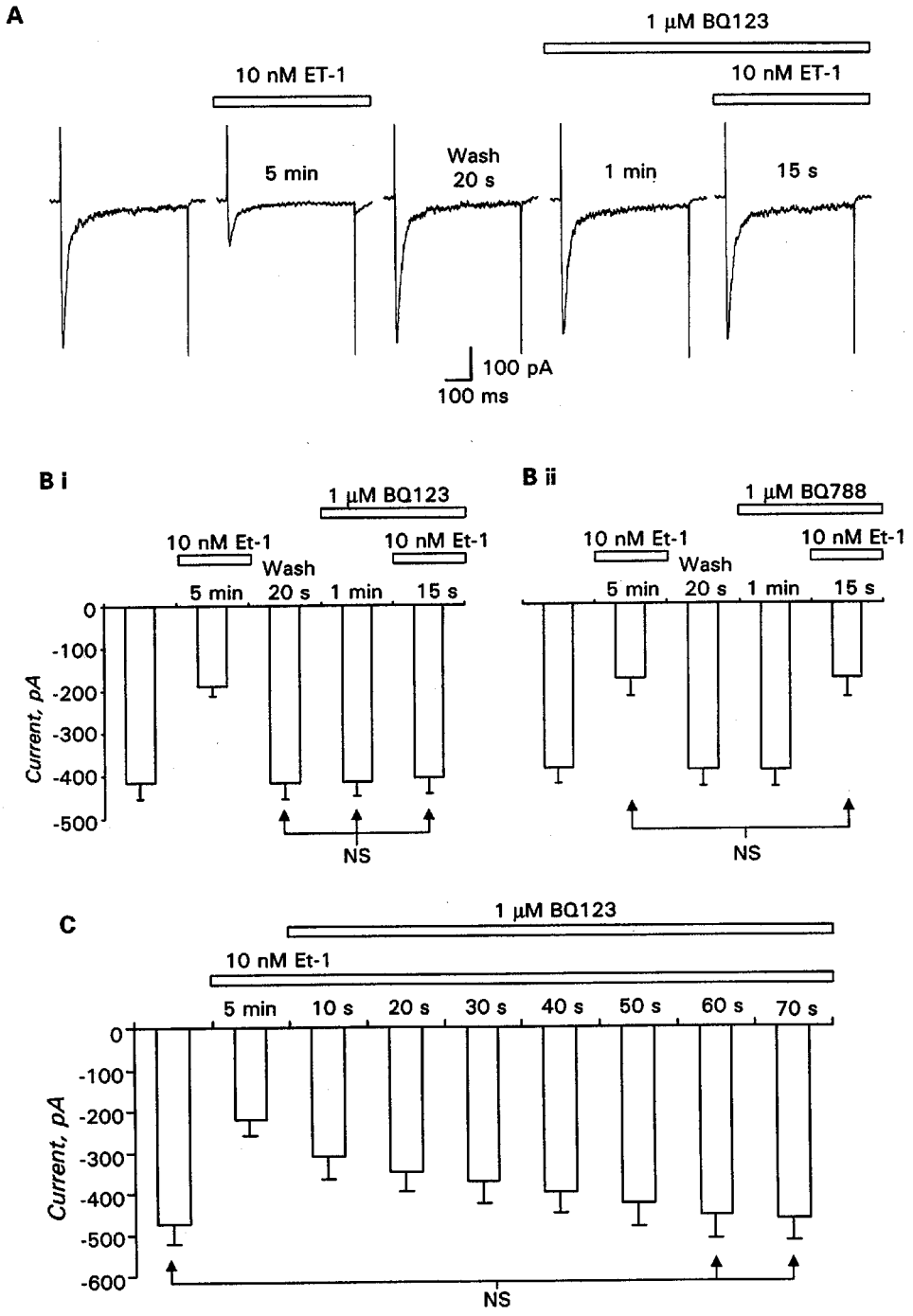

Figure 4 Effect of BQ123 and BQ788 on the blockade of $I_{Ca(L)Na}$ by Et-1 (A) Current record for a vessel fragment in response to voltage steps to −20 mV from a holding potential of −80 mV showing that the Et_A receptor antagonist BQ123 (1 μM) prevents the inhibition of $I_{Ca(L)Na}$ by 10 nM Et-1. It was necessary to firstly confirm a sustained block of $I_{Ca(L)Na}$ by Et-1 prior to testing the effects of the antagonist (see text). (Bi) Pooled data from six similar experiments, where the NS labels are P values of >0.05 for BQ123 and BQ123 plus Et-1 against wash Et-1. (Bii) These experiments were repeated with the Et_B receptor antagonist BQ788. This peptide failed to prevent the inhibition of $I_{Ca(L)Na}$ by Et-1 ($n=4$). (C) Histograms showing that BQ123 (1 μM) reverses the depression of $I_{Ca(L)Na}$ by Et-1 (voltage steps were again from −80 to −20 mV in divalent free medium). Current values at 60 and 70 s BQ123 plus Et-1 were not significantly different ($P>0.05$) from those recorded prior to the application Et-1, as indicated by the NS labels.

washout. Upon re-application of ABT-627 the level of depression seen was the same as that achieved with 5–10 min exposure to the antagonist. Subsequently, we examined whether the blockade of $I_{Ca(L)Na}$ by ABT-627 prevented any further effect by Et-1 (Figure 5B). Within the same vessels the level of inhibition of $I_{Ca(L)Na}$ observed was the same with Et-1 or ABT-627 applied individually and no significant increase in the blockade occurred when the two

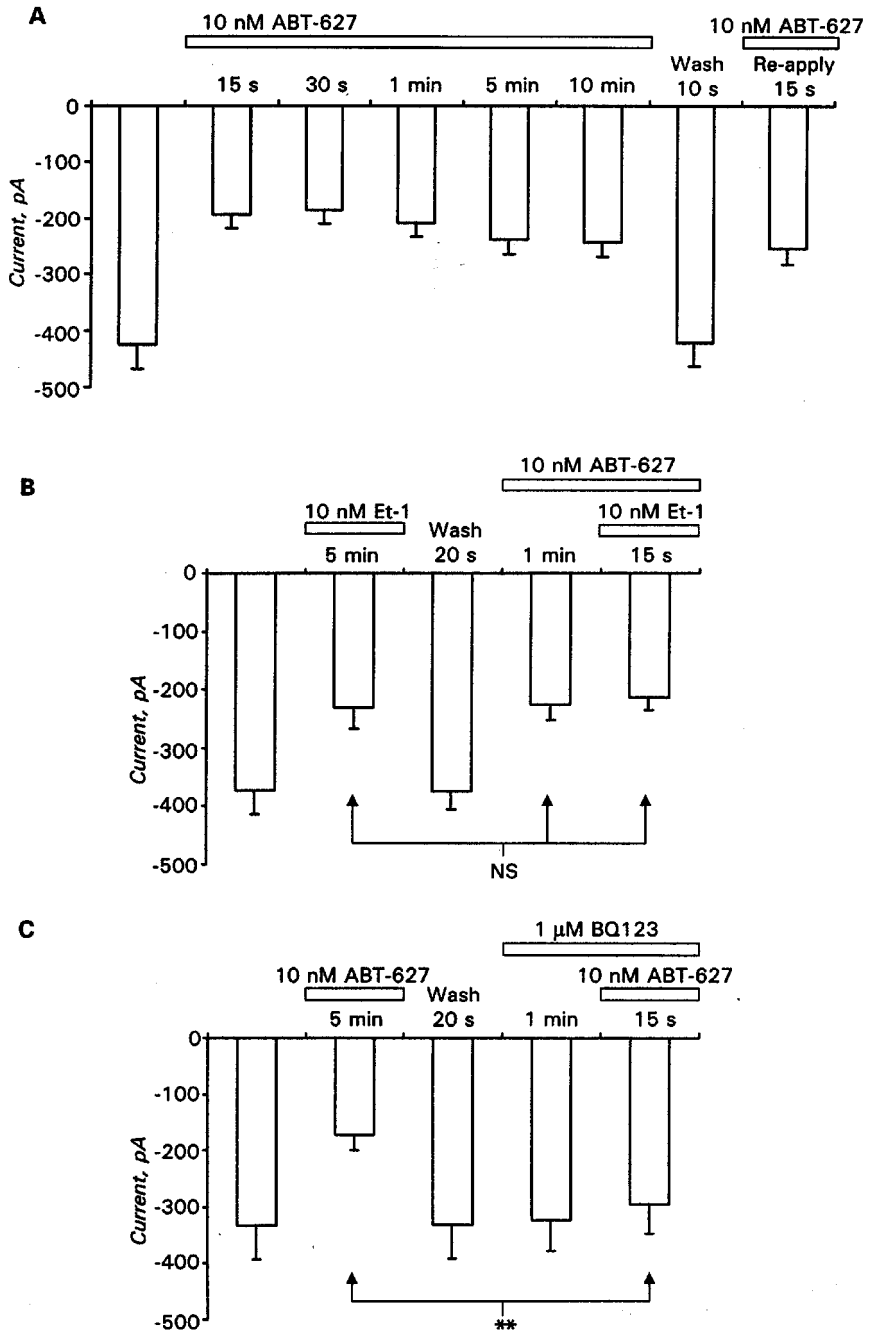

Figure 5 ABT-627 as an agonist on the Ca^{2+} channel inhibition. (A) Histogram constructed from five vessel recordings showing the time course for the inhibition of $I_{Ca(L)Na}$ by ABT-627. Note that the pattern of inhibition is identical to that seen with Et-1 in Figure 3Aii. Voltage steps were again from −80 to −20 mV in divalent free solution. (B) Experiments described in Figure 4Bi,ii were repeated, but this time with ABT-627. NS are *P*-values of >0.05 for ABT-627 and ABT-627 plus 10 nM Et-1 versus Et-1 ($n=4$). (C) Histogram showing that BQ123 blocks the inhibition of $I_{Ca(L)Na}$ by ABT-627 ($n=5$). **Indicates a *P* value of <0.01 for BQ123 plus ABT-627 against ABT-627.

compounds were used together. These data suggested that ABT-627 might be acting as an agonist on the Ca^{2+} channel inhibition and the final experiments sought to explore this further. Specifically, we tested whether BQ123 was capable of preventing the sustained inhibition of $I_{Ca(L)Na}$ by ABT-627 (Figure 5C). Nearly all of the block of $I_{Ca(L)Na}$ by ABT-627 was inhibited by BQ123.

Discussion

These experiments provide both functional and pharmacological evidence for two co-existing Et_A receptor subtypes in rabbit choroidal arteriolar smooth muscle.

The activation of $I_{Cl(Ca)}$ is *via* a classical Et_A receptor since it persists whether or not Et-1 is washed out and is associated

with a persistent rise in cell Ca and sustained contraction (Curtis & Scholfield, 2001). In the present experiments, the Et_A receptor antagonists BQ123 and ABT-627 were able to prevent the effect, but they failed to inhibit the oscillatory Cl^- currents once they had been set in train. The most likely explanation for these results is that binding of Et-1 its receptor is practically irreversible. Indeed, binding studies have shown that Et-1 dissociates from its receptors extremely slowly with a half time of >30 h at 37°C in vascular smooth muscle (Waggoner *et al*., 1992). This tight binding causes a continual activation of the relevant G-protein and associated messenger pathway(s), which persists even after the receptor has been internalized (Chun *et al*., 1995). It is believed that the persistence of Et-1 binding is due to an abrupt change in the Et/Et_A receptor complex, which greatly increases ligand affinity and that this occurs prior to formation of the active G-protein associated complex (Hilal-Dandan *et al*., 1997). Thus, irreversibility would not seem to be determined by the type of G-protein to which the Et_A receptor is coupled.

A striking feature of the Ca^{2+} channel inhibition was its rapid reversal, which occurred within 10 s of washing out Et-1 or 60 s of applying BQ123 concurrent with Et-1. This contrasts markedly with the apparent irreversible activation of $I_{Cl(Ca)}$. Thus it seems that the Ca^{2+} channel inhibition is mediated through an atypical receptor variant that does not convert into a high affinity state.

The pharmacology also indicates that the activation of the $I_{Cl(Ca)}$ and inhibition of Ca^{2+} channels are mediated through different Et_A receptor subtypes. BQ123 and ABT-627 are regarded as competitive and selective Et_A antagonists and they both blocked the persistent effect of Et-1. However, the effect of ABT-627 on $I_{Ca(L)Na}$ was completely different: it mimicked Et-1 as an agonist and its action was blocked by BQ123.

The idea of heterogeneity among Et_A receptors is not entirely new. In rabbit saphenous vein two types of Et_A receptor have been postulated (Sudjarwo *et al*., 1994) but this was based on differential sensitivities to BQ123. However, for Et_B receptors there is much clearer evidence for distinct molecular moieties since two gene products have been identified. Our current findings may reflect an entirely separate gene product or more likely some type of splice variant of which several have been identified (Miyamoto *et al*., 1996; Bourgeois *et al*., 1997).

In conclusion, these experiments have shown that Et-1, *via* Et_A receptors, irreversibly activates $I_{Cl(Ca)}$ and reversibly inhibits L-type Ca^{2+} channels in the rabbit choroidal arteriolar smooth muscle. It is suggested that two Et_A receptor subtypes may exist within this tissue and further work should now be conducted with a view of characterizing these receptor variants at a molecular level.

We thank the Wellcome Trust and the British Heart Foundation for financial support.

References

ARAI, H., HORI, S., ARAMORI, I., OHKUBO, H. & NAKANISHI, S. (1990). Cloning and expression of a cDNA encoding an endothelin receptor. *Nature,* **348,** 730–732.

BOURGEOIS, C., ROBERT, B., REBOURCET, R., MONDON, F., MIGNOT, T.M., DUC-GOIRAN, P. & FERRE, F. (1997). Endothelin-1 and ETA receptor expression in vascular smooth muscle cells from human placenta: a new ETA receptor messenger ribonucleic acid is generated by alternative splicing of exon 3. *J. Clin. Endocrinol. Metab.,* **82,** 3116–3123.

BURSELL, S.E., CLERMONT, A.C., OREN, B. & KING, G.L. (1995). The in vivo effect of endothelins on retinal circulation in nondiabetic and diabetic rats. *Invest. Ophthalmol. Vis. Sci.,* **36,** 596–607.

CHAKRAVARTHY, U., MCGINTY, A., MCKILLOP, J., ANDERSON, P., ARCHER, D.B. & TRIMBLE, E.R. (1994). Altered endothelin-1 induced contraction and second messenger generation in bovine retinal microvascular pericytes cultured in high glucose medium. *Diabetologia,* **37,** 36–42.

CHUN, M., LIN, H.Y., HENIS, Y.I. & LODISH, H.F. (1995). Endothelin-induced endocytosis of cell surface ET_A receptors. Endothelin remains intact and bound to the ET_A receptor. *J. Biol. Chem.,* **270,** 10855–10860.

CURTIS, T.M. & SCHOLFIELD, C.N. (1999). Endothelin blocks L-type calcium channels in microvascular smooth muscle of the rabbit choroid. *Br. J. Pharmacol.,* **127,** 9P.

CURTIS, T.M. & SCHOLFIELD, C.N. (2000). Transient Ca^{2+}-activated Cl-currents with endothelin in isolated arteriolar smooth muscle cells of the choroid. *Invest. Ophthalmol. Vis. Sci.,* **41,** 2279–2285.

CURTIS, T.M. & SCHOLFIELD, C.N. (2001). Nifedipine blocks Ca^{2+} store refilling through a pathway not involving L-type Ca^{2+} channels in rabbit arteriolar smooth muscle. *J. Physiol.,* **532,** 609–623.

DE LA RUBIA, G., OLIVER, F.J., INOGUCHI, T. & KING, G.L. (1992). Induction of resistance to endothelin-1's biochemical actions by elevated glucose levels in retinal pericytes. *Diabetes,* **41,** 1533–1539.

GUIBERT, C. & BEECH, D.J. (1999). Positive and negative coupling of the endothelin ET_A receptor to Ca^{2+}-permeable channels in rabbit cerebral cortex arterioles. *J. Physiol.,* **514,** 843–856.

HAMILL, O.P., MARTY, A., NEHER, E., SAKMANN, B. & SIGWORTH, F.J. (1981). Improved patch-clamp techniques for high-resolution current recording from cells and cell-free membrane patches. *Pflügers Arch.,* **391,** 85–100.

HILAL-DANDAN, R., VILLEGAS, S., GONZALEZ, A. & BRUNTON, L.L. (1997). The quasi-irreversible nature of endothelin binding and G protein-linked signaling in cardiac myocytes. *J. Pharmacol. Exp. Ther.,* **281,** 267–273.

HORN, R. & MARTY, A. (1988). Muscarinic activation of ionic currents measured by a new whole-cell recording method. *J. Gen. Physiol.,* **92,** 145–159.

LAMPL, Y., FLEMINGER, G., GILAD, R., GALRON, R., SAROVA-PINHAS, I. & SOKOLOVSKY, M. (1997). Endothelin in cerebrospinal fluid and plasma of patients in the early stage of ischemic stroke. *Stroke,* **28,** 1951–1955.

LARGE, W.A. & WANG, Q. (1996). Characteristics and physiological role of the Ca^{2+}-activated Cl-conductance in smooth muscle. *Am. J. Physiol.,* **271,** C435–C454.

MCDONALD, T.F., PELZER, S., TRAUTWEIN, W. & PELZER, D.J. (1994). Regulation and modulation of calcium channels in cardiac, skeletal, and smooth muscle cells. *Physiol. Rev.,* **74,** 365–507.

MCGINTY, A., SCHOLFIELD, C.N., LIU, W.H., ANDERSON, P., HOEY, D.E. & TRIMBLE, E.R. (1999). Effect of glucose on endothelin-1-induced calcium transients in cultured bovine retinal pericytes. *J. Biol. Chem.,* **274,** 25250–25253.

MIYAMOTO, Y., YOSHIMASA, T., ARAI, H., TAKAYA, K., OGAWA, Y., ITOH, H. & NAKAO, K. (1996). Alternative RNA splicing of the human endothelin-A receptor generates multiple transcripts. *Biochem. J.,* **313,** 795–801.

PLUTA, R.M., BOOCK, R.J., AFSHAR, J.K., CLOUSE, K., BACIC, M., EHRENREICH, H. & OLDFIELD, E.H. (1997). Source and cause of endothelin-1 release into cerebrospinal fluid after subarachnoid hemorrhage. *J. Neurosurg.,* **87,** 287 – 293.

SAKURAI, T., YANAGISAWA, M., TAKUWA, Y., MIYAZAKI, H., KIMURA, S., GOTO, K. & MASAKI, T. (1990). Cloning of a cDNA encoding a non-isopeptide-selective subtype of the endothelin receptor. *Nature,* **348,** 732 – 735.

STITT, A.W., CHAKRAVARTHY, U., GARDINER, T.A. & ARCHER, D.B. (1996). Endothelin-like immunoreactivity and receptor binding in the choroid and retina. *Curr. Eye. Res.,* **15,** 111 – 117.

SUDJARWO, S.A., HORI, M., TANAKA, T., MATSUDA, Y., OKADA, T. & KARAKI, H. (1994). Subtypes of endothelin ET_A and ET_B receptors mediating venous smooth muscle contraction. *Biochem. Biophys. Res. Commun.,* **200,** 627 – 633.

WAGGONER, W.G., GENOVA, S.L. & RASH, V.A. (1992). Kinetic analyses demonstrate that the equilibrium assumption does not apply to $^{[125I]}$endothelin-1 binding data. *Life Sci.,* **51,** 1869 – 1876.

WEBB, D.J., MONGE, J.C., RABELINK, T.J. & YANAGISAWA, M. (1998). Endothelin: new discoveries and rapid progress in the clinic. *Trends Pharmacol. Sci.,* **19,** 5 – 8.

YANAGISAWA, M., KURIHARA, H., KIMURA, S., TOMOBE, Y., KOBAYASHI, M., MITSUI, Y., YAZAKI, Y., GOTO, K. & MASAKI, T. (1988). A novel potent vasoconstrictor peptide produced by vascular endothelial cells. *Nature,* **332,** 411 – 415.

(Received September 9, 2001
Accepted September 18, 2001)